Brain Struct Funct (2016) 221:4111–4127
DOI 10.1007/s00429-015-1151-3

ORIGINAL ARTICLE

The expression of SEIPIN in the mouse central nervous system

Xiaoyun Liu[1] · Beibei Xie[2] · Yanfei Qi[1] · Ximing Du[1] · Shaoshi Wang[3] · Yumei Zhang[4] · George Paxinos[5,6] · Hongyuan Yang[1] · Huazheng Liang[5,6]

Received: 31 July 2015 / Accepted: 19 November 2015 / Published online: 30 November 2015

Abstract Immunohistochemical staining was used to investigate the expression pattern of SEIPIN in the mouse central nervous system. SEIPIN was found to be present in a large number of areas, including the motor and somatosensory cortex, the thalamic nuclei, the hypothalamic nuclei, the mesencephalic nuclei, some cranial motor nuclei, the reticular formation of the brainstem, and the vestibular complex. Double labeling with NeuN antibody confirmed that SEIPIN-positive cells in some nuclei were neurons. Retrograde tracer injections into the spinal cord revealed that SEIPIN-positive neurons in the motor and somatosensory cortex and other movement related nuclei project to the mouse spinal cord. The present study found more nuclei positive for SEIPIN than shown using in situ hybridization and confirmed the presence of SEIPIN in neurons projecting to the spinal cord. The results of this study help to explain the clinical manifestations of patients with Berardinelli–Seip congenital lipodystrophy (Bscl2) gene mutations.

Keywords SEIPIN · Brain · Supraspinal projection · Spinal cord · Seipinopathy · Motor control

✉ Hongyuan Yang
h.rob.yang@unsw.edu.au

✉ Huazheng Liang
h.liang@neura.edu.au; a.liang@neura.edu.au

[1] School of Biotechnology and Biomolecular Sciences, The University of New South Wales, NSW, Australia

[2] Department of Gynecology and Obstetrics, Linyi Hospital, Linyi, Shangdong Province, China

[3] Department of Neurology, Shanghai No. 1 People's Hospital, Shanghai, China

[4] Department of Neurology, Beijing Tiantan Hospital, Capital Medical University, Beijing, China

[5] Neuroscience Research Australia, 139 Barker Street, Randwick, NSW 2031, Australia

[6] School of Medical Sciences, The University of New South Wales, Kensington, NSW, Australia

Introduction

SEIPIN is a membrane protein of the endoplasmic reticulum (ER), encoded by the Berardinelli–Seip congenital lipodystrophy (Bscl2) gene, which is located on chromosome 11q13 (Magre et al. 2001; Fei et al. 2011). The 462 amino acid long protein is the predominant form after translation compared with the 398 residues long protein, with both N- and C-terminals facing the cytoplasm and the only helix facing the ER lumen (Lundin et al. 2006). Gain-of-function mutations result in distal hereditary motor neuropathy and Silver syndrome (Silver 1966; Magre et al. 2001; Irobi et al. 2004; Windpassinger et al. 2004; Guillén-Navarro et al. 2013), whereas loss-of-function mutations cause type 2 congenital generalized lipodystrophy (Ebihara et al. 2004; Cui et al. 2011). The expression of the Bscl2 gene was localized to a range of tissues, with the brain and the testis having the highest expression level (Magre et al. 2001). In the central nervous system, not only the brain but also the spinal cord expresses this gene (Windpassinger et al. 2003; Ito and Suzuki 2007; Ito et al. 2008a, b). This explains the involvement of peripheral nerves in the neuropathy as evidenced by the atrophy and wasting of distal limb muscles (Windpassinger et al. 2003). In neuronal cells SEIPIN is expressed in the aggresomes when fused with a reporter gene GFP. The degradation of the SEIPIN protein follows the aggresome pathway. Aggresome formation occurs in some neurodegenerative diseases (Ito et al.

2008a, b) and it was also observed that mutant SEIPIN proteins induce apoptosis or motor neuron loss (Ito and Suzuki 2007; Guo et al. 2013). However, neuronal loss is not necessarily present in neurodegenerative diseases as shown by the mutant SEIPIN tg mouse (Yagi et al. 2011). This suggests that SEIPIN has a role in CNS degeneration. One of the mechanisms might be the dysregulation of excitatory synaptic transmission (Wei et al. 2013, 2014). To understand how this protein works, studies have started using a SEIPIN antibody to test the anatomical expression of SEIPIN in motor neurons of the spinal cord, cortical neurons in the frontal lobe, the pituitary gland, the paraventricular nucleus of the hypothalamus, the nucleus of vagus, and the solitary nucleus (Ito and Suzuki 2007; Ito et al. 2008a, b; Garfield et al. 2012). However, the detailed information about its anatomical expression comes from in situ hybridization against the Bscl2 gene (Garfield et al. 2012), from which a large number of nuclei have been reported to have Bscl2 mRNA. Due to the limitations of this technique, some weakly positive cells or widely spread cells might have been missed in this report. The present study aimed to thoroughly map the expression of SEIPIN in the central nervous system using a recently developed, highly specific antibody against SEIPIN (Jiang et al. 2014).

Materials and methods

Animals

Fourteen C57/BL6 mice, 10–12 weeks of age and 25–30 g in weight, were used for this study. These mice were obtained from the Animal Resource Center in Western Australia. The experimental procedures were approved by the Animal Care and Ethics Committee of The University of New South Wales (approval number 14/94A).

Retrograde tracing

Mice were anaesthetized with an intraperitoneal injection of ketamine (80 mg/kg) and xylazine (5 mg/kg) and placed in a mouse stereotaxic head holder (Kopf Instruments, Tujunga, CA, USA). The ear bars were carefully tightened to stabilize the mouse head. After shaving the fur and sterilizing the skin, spinal cord segments were exposed by making an incision along the midline of the neck and performing a laminectomy at C3 or C4. The dura mater on the right side of the spinal cord was penetrated with the tip of a 29-gauge insulin injection needle and then the needle of a 5 μL Hamilton syringe (Hamilton Company, Reno, NV, USA; the outer diameter is 0.711 mm) was driven through this opening. Twenty to 40 nL of fluoro-gold (FG) (Fluorochrome, Denver, Co, USA; diluted to 5 % in distilled water) solution was injected through the needle into the right side of the spinal cord. The needle of the Hamilton syringe was left in place for 10 min after the injection. In the present study, five mice were injected with fluoro-gold into the cervical spinal cord. In the control group, two mice received normal saline injections into the spinal cord (sham group) and another two mice received fluoro-gold injections into the cisterna magna to exclude the transportation of fluoro-gold through cerebrospinal fluid. After fluoro-gold injections, the soft tissue and the skin were sutured and an antibiotic—tetracycline (Pfizer)—was applied topically over the incision. Buprenorphine (Temgesic, Reckitt Benckiser) solution was injected to relieve pain.

Tissue preparation

After 4 days by which time the tracer had reached its target, all mice were anesthetized with a lethal dose of sodium pentobarbital solution (0.1 mL, 200 mg/mL) and perfused as described previously (Liang et al. 2011). Brains and spinal cords were removed and postfixed in 4 % paraformaldehyde for 2 h at 4 °C, followed by cryoprotection in 30 % sucrose in 0.1 M PB solution overnight at 4 °C. Serial sections of the brain and spinal cord were cut at 40 μm using a Leica CM 1950 cryostat. Five mice that did not undergo surgery were perfused and cut in the same way as mentioned above.

Immunohistochemical/immunofluorescence staining

Peroxidase immunohistochemistry for SEIPIN was undertaken on half of the brain and spinal cord sections of the five mice that did not undergo surgery, and immunofluorescent staining for NeuN on the other half. The first half were washed and treated with 1 % H_2O_2 in 50 % ethanol before being transferred into 5 % goat serum in 0.1 M PB to block non-specific antigen binding sites. The sections were incubated in the primary anti-SEIPIN (a gift from Prof Jiahao Sha, 1:500; raised in rabbit) solution overnight and subsequently in the secondary antibody (biotinylated goat anti-rabbit IgG; Sigma, 1:200) for 2 h. The sections were then washed and transferred to an extravidin peroxidase solution (Sigma, 1:1000) for 2 h. Finally, the sections were incubated in a 3,3,-diaminobenzidine (DAB) reaction complex (Vector lab, Burlingame, CA, USA) until an optimal colour developed. At the end of the procedure, the sections were mounted and dehydrated before being coverslipped. The other half of the sections, used for immunofluorescence staining, were incubated in a primary antibody solution containing NeuN (1:500, Merck Millipore, MAB2300, raised in mouse) and SEIPIN. The secondary antibodies were goat anti-mouse Alexa Fluor 488

and goat anti-rabbit Alexa Fluor 594 for NeuN and SEIPIN, respectively.

For the nine mice that received either tracer injection or sham injection; half of their brain and spinal cord sections were stained for Nissl, and the other half for SEIPIN immunofluorescence. In the latter experiment, the same protocol as above was used.

Western blot analysis

Protein extracted from the white adipose tissue of the C57BL/6 wild type and the Seipin−/− colony (generated in C57BL/6 background) was given as a gift by Prof Jiahao Sha. The protein concentration was determined using a bicinchoninic acid protein assay kit (Sigma, Sydney, Australia), and 40 µg of protein was analyzed using a 4–12 % NuPAGE® Bis–Tris Precast Gel (Life Technologies, Mulgrave, Australia). The antibody against SEIPIN was generated by Prof Jiahao Sha (Jiang et al. 2014), and anti-β-ACTIN was purchased from Sigma. Western Blot images were captured by ChemiDocTM XRS + (Bio-Rad, Gladesville, Australia).

Data analysis

DAB stained mouse brain and spinal cord sections were scanned with an Aperio slide scanner (ScanScope XT™, Leica Biosystems) under 200× magnification. Scanned images were opened with ImageScope and various magnifications extracted from the "virtual slide". Fluorescent signals were detected with a Nikon fluorescent microscope equipped with Stereoinvestigator™ software. Images were taken from different channels and merged automatically. The brightness and contrast of these images were then modified with Adobe Photoshop CS6 and organized with Adobe Illustrator CS6. The mouse brain sections were then compared with a mouse brain atlas (Paxinos and Franklin 2013). The spinal cord sections were compared with a spinal cord atlas (Sengul et al. 2012).

Results

SEIPIN was present in the white adipose tissue of the C57BL/6 mouse, but not present in that of the *Seipin*$^{-/-}$ mouse (Fig. 1). This showed the specificity of the antibody.

SEIPIN expression was found in brain nuclei along the entire rostrocaudal neural axis. While the majority of the brain nuclei expressed low to moderate levels of SEIPIN, a few nuclei expressed high levels of this protein (see the list of nuclei positive for SEIPIN in Table 1). The abbreviations of the names of brain areas were adopted from the mouse brain atlas (Paxinos and Franklin 2013).

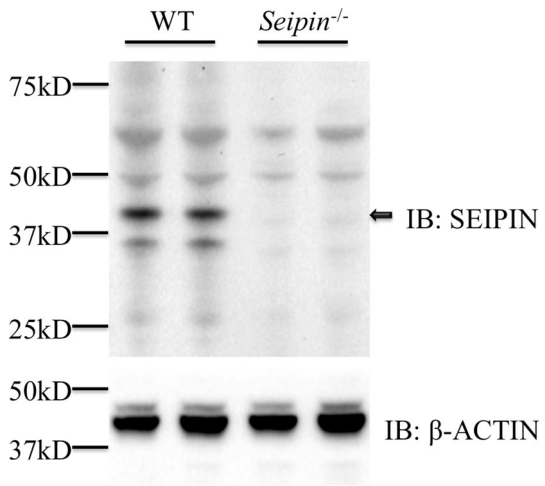

Fig. 1 Western blot showing the specificity of SEIPIN antibody. *Arrow* indicates the endogenous mouse SEIPIN at ~43 kD

In the forebrain, SEIPIN expression was found in the majority of the cortical areas, although its expression was not even throughout. While most of the cortical areas expressed low to moderate levels of SEIPIN, the motor, frontal association cortex, piriform cortex, cingulate cortex, area 24b, dorsal and ventral parts of the agranular insular cortex, the dorsolateral entorhinal cortex, temporal association cortex, ectorhinal cortex/perirhinal cortex showed moderate to high levels of expression. Positive neurons in the anterior olfactory nucleus were randomly distributed (Figs. 2a, 3a). Throughout the secondary motor cortex, positive cells were in layers 4, 5 and 6, whereas the primary motor cortex mainly had positive neurons in layer 4 and 6 (Figs. 2a–c, 3b). Consequently there was observed to be a gap between SEIPIN-positive cells in layer 4 and 6. This gap was smaller in the adjacent agranular insular and orbital cortices than in the primary motor cortex (Fig. 2a–e). A distinctive characteristic of the S1 was the presence of fewer neurons in layer 6 (Figs. 2b–f, 3c). In the caudal part of the agranular insular cortex, there were few positive cells in layer 4, which was distinct from the secondary somatosensory cortex and the piriform cortex (Fig. 2c–e). This was also the case in the granular and dysgranular insular cortices and the ectorhinal and perirhinal cortices (Fig. 2f–i). In the hippocampus, a small number of positive cells were found in the oriens and pyramidal layers and the stratum lucidum in the rostral portion of it (Figs. 2f–i, 3g). There were more positive cells in the caudal portion of it (Table 2).

In the subcortical areas, the dorsal/ventral tenia tecta, medial septal nucleus, ventral part of the lateral septal nucleus, nucleus of the ventral/horizontal limb of the diagonal band, ventral pallidum, globus pallidus, and the posterodorsal/posteroventral part of the medial amygdaloid nucleus had moderate to high levels of SEIPIN expression, whereas the caudate putamen, accumbens nucleus (except

Table 1 Expression of SEIPIN in brain areas

Brain area	Expression level	Brain area	Expression level
FrA	++~+++	MeAD/MeAV	+~++
A32	++	CeM/CeL	+~++
DLO	++	A29c/A30	+~++
LO	++	Hip	+
VO/MO	~+	MD/PC/CL/Sub	+~++
AOM	+	PaPo	+++
Gl	~+	VMHDM	+++~++++
AOD/AOL/AOV	~+	EP	~+
M1/M2	++~+++	VPL/VPM	++~+++
Fr3	+~++	ZI	++~+++
AID/AIV	+++	VMHVL/VMHC	++~+++
S1 J	++~+++	Ect/PRh	++~+++
DTT	++~+++	MePD/MePV	++
Pir	++~+++	DLG	+++
A24b	++~+++	Po	++~+++
GI/DI	++	STh	++
CPu	~+	DM	++~+++
AcbC	~+	DA/Xi/Re	++
AcbSh	++~+++	PVP	~+
LSI/LSD	+~++	PaF/PC/OPC	++~+++
DEn	~+	PH	++
IEn	+~++	SPF	++
LSV	~+	DLG/PrGMC	++~+++
S1FL/S1 J/S1DZ/S1ULp	++	p1PAG/PrC	++
Cl	~+	PR	~+
MS	++~+++	F	+~++
VDB/HDB	++~+++	PMV/PMD	+~++
LDB	+~++	Arc	++++
VP	+++	V1	~+
LPO/MPA	+~++	V2MM/V2ML	++
SIB	~+	V2L	+~++
IPACL/IPACM	~+	AuD/AuV/Au1	++
SHy	+++	DLEnt/TeA	++~+++
STMA/STLP	+~++	AHiPM/PMCo/PLCo	+~++
STLJ/STLD	+~++	PR	+
MPO	+++~++++	Lth/MCPC	+~++
PVA	~+	RPF	+
SchDL	+	CLi	~+
Re	+	SubG	+
PaAP	+++	SNR/SNL/SNC	+~+++
AHA	+~++	RMM/RML	++
LA	+++	RMC/RPC	++~+++
LH	+++	InWh/DpG	+~++
GP	++	DK/MA3	+
EA	+	3 N	++~+++
AA	++	mRt	+
LOT	++~+++	BIC	+
ACo	+~++	IP	++
CxA	~+	PIF	+
AD/AV	+~++	SubB	+~++

Table 1 continued

Brain area	Expression level	Brain area	Expression level
Rt	~+	PnO	+~++
Pe	+++	Pn	+~++
PaMP	+++	PL	+~++
PaDC/PaLM	+++~++++	MnR/PMnR	+
BMA	+~++	4 N/Pa4	++
BLA	~+	RtTg	++
LDDM	+~++	PBG/MiTg	+
VM/VL	+~++	BIC/ECIC	+
EW	+~++	SuVe/VeCb/SpVe	~+
MPB/LPB	+	DPGi/Gi/LPGi/GiA/GiV	+~++
PrCnF	~+	PPy	++
AHC/AHP	++~+++	Lat/Med/IntA/IntP	+~++
MnR/DR	++	SGe/Pr	++
VTg	++	PCRt/IRt/Li	+
Tz/DC	+~++	RMg/RPa	~+
CAT	+	Amb	+~++
PnC/SubC	+~++	PrBo/CVL	+~++
Pr5/Sp5	~+	12 N/Ro	+++
5 N/6 N/7 N	++~+++	IO	+
LDTg/Bar/PDTg/CGB	+	MdD/MdV	~+
LC	+++	10 N/AP	++
MVe	+~++	ECu	+~++
LVe	++	LRt	+~++

shell region which had moderate levels of expression), basal part of the substantia innominata, lateral/medial part of the interstitial nucleus of the posterior limb of the anterior commissure, and the extension of the amygdala had low levels of SEIPIN expression (Fig. 2b–f). Positive cells in the caudate putamen were mainly in the ventral part (Figs. 2b–f, 3d). These SEIPIN-positive cells were continuous with those in the central amyloid nucleus, whose density of positive cells was also low (Figs. 2d, e, 3e).

In the thalamus, most of the nuclei expressed low to moderate levels of SEIPIN (including anterodorsal/anteroventral thalamic nucleus, reuniens thalamic nucleus, ventromedial/ventrolateral thalamic nucleus, mediodorsal/paracentral/centrolateral/submedius thalamic nucleus, xiphoid thalamic nucleus, subgeniculate nucleus of prethalamus, posterior part of the paraventricular thalamic nucleus), but the anterior part of the paraventricular thalamic nucleus, ventral posteromedial/posterolateral thalamic nucleus, zona incerta, dorsal lateral geniculate nucleus, magnocellular part of the pregeniculate nucleus of the prethalamus, parafascicular thalamic nucleus/oval paracentral thalamic nucleus showed moderate to high levels of SEIPIN expression (Fig. 2d–f). In ventral posteromedial and posterolateral thalamic nuclei, the density of positive cells was high but the intensity of labeling was lower than those in dorsal lateral geniculate nucleus (Fig. 2g).

In the hypothalamus, a number of nuclei such as septohypothalamic nucleus, medial preoptic nucleus, anterior parvicellular/medial parvicellular/dorsal cap/lateral magnocellular/posterior part of the paraventricular hypothalamic nucleus, lateroanterior hypothalamic nucleus, lateral hypothalamic area, dorsomedial part of the ventromedial hypothalamic nucleus, arcuate hypothalamic nucleus, and the medial part of the retromammillary nucleus expressed high levels of SEIPIN (Figs. 2d–i, 3f, h). Only a small number of nuclei expressed low to moderate levels, including dorsal hypothalamic area, subthalamic nucleus, anterior/posterior/central part of the anterior hypothalamic area, lateral/medial preoptic area, dorsal/ventral part of the premammillary nucleus (Fig. 2d–i).

In the pretectum, prosomere 1 periaqueductal gray, precommissural nucleus, magnocellular nucleus of the posterior commissure, lethoid nucleus, nucleus of the fields of Forel, prerubral field, retroparafascicular nucleus, nucleus of Darkschewitsch, medial accessory oculomotor nucleus expressed low to moderate levels of SEIPIN (Fig. 2g–i).

In the midbrain, the intermediate white and deep gray layers of the superior colliculus, the mesencephalic reticular formation, nucleus of the brachium/external cortex of the inferior colliculus, precuneiform nucleus, median raphe nucleus, and the dorsal raphe nucleus expressed low to

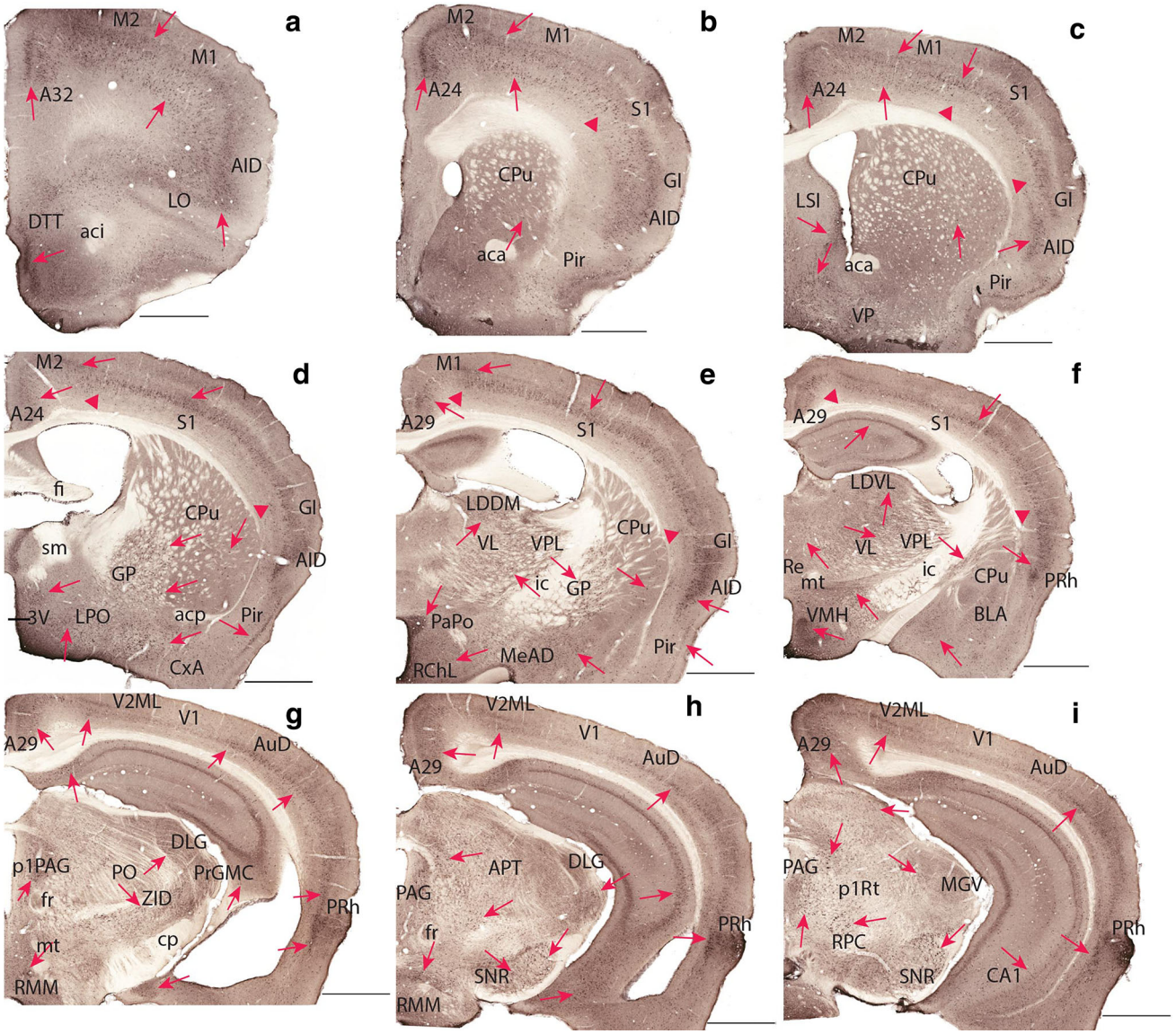

moderate levels of SEIPIN, whereas the magnocellular and parvicellular parts of the red nucleus, reticular/lateral part of the substantia nigra, and the oculomotor nucleus expressed moderate to high levels of SEIPIN (Fig. 2h–l). In the superior colliculus, positive cells were mainly found in the ventrolateral part of the intermediate white and deep gray layers of the superior colliculus (Fig. 2j, k). Positive cells in the magnocellular part of the red nucleus were mainly found in the caudal portion of this nucleus. So were positive cells in the substantia nigra (Figs. 2h–j, 3i, j).

In the hindbrain, the oral and caudal parts of pontine reticular nucleus, pontine nuclei, paralemniscal nucleus, nucleus of the trapezoid body, Barrington's nucleus, laterodorsal tegmental nucleus, lateral, medial, superior and the spinal vestibular nuclei, vestibulocerebellar nucleus, gigantocellular reticular nucleus, the lateral paragigantocellular reticular nucleus, lateral, medial, and interposed cerebellar nuclei, supragenual nucleus, parvicellular and intermediate reticular nuclei, raphe magnus and pallidus nuclei, inferior olive, dorsal and ventral parts of medullary reticular nucleus, external cuneate nucleus, and the lateral reticular nucleus expressed low to moderate levels of SEIPIN (Fig. 2m–r). A small number of nuclei expressed moderate levels of SEIPIN, including the trochlear nucleus, paratrochlear nucleus, ventral tegmental nucleus, vagus nerve nucleus, and the area postrema. In contrast, the locus coeruleus, motor trigeminal nucleus, abducens nucleus, facial nucleus, hypoglossal nucleus and the nucleus of Roller expressed high levels of SEIPIN (Fig. 2k–m, q, r). In the oral part of pontine reticular nucleus, positive cells were mainly found in the central portion, mediolaterally (Fig. 2k, l), whereas positive cells in the gigantocellular reticular nucleus were mainly found in its ventral portion (Fig. 2m–q). The lateral vestibular

◀**Fig. 2** Expression of SEIPIN in the mouse brain and spinal cord shown by immunohistochemical staining with the SEIPIN antibody. Details are found in Table 1. **a–r** SEIPIN-positive neurons were present in the motor (M1 and M2) and somatosensory (S1 and S2, *between the two triangles*) cortices, the A32 and A24 areas, the piriform cortex, the visual and auditory cortical areas, the perirhinal cortex, the anterior olfactory nuclei, the dorsal tenia tecta (DTT), the orbital cortex (LO), granular and dysgranular insular cortex (GI and DI), the septum (LSI), the caudate putamen (CPu), the globus pallidus (GP), the ventral pallidum (VP), the nucleus of the vertical limb of the diagonal band (VDB) and the nucleus of the horizontal limb of the diagonal band (HDB), the medial septal nucleus (MS), the amygdaloidal areas including the cortex-amygdala transition zone (CxA), the basolateral amygdaloid nucleus (BLA), the medial amygdaloid nucleus (MeAD), the anterior hypothalamic area, the lateral preoptic nucleus (LPO), the posterior paraventricular nucleus (PaPo), the lateral retrochiasmatic area (RChL), the thalamic nuclei including the ventral posterolateral thalamic nucleus (VPL), the ventrolateral thalamic nucleus (VL), the reuniens thalamic nucleus (Re), the dorsomedial and ventrolateral parts of the laterodorsal thalamic nucleus (LDDM/LDVL), the dorsolateral geniculate nucleus (DLG) and the medial geniculate (MG), the magnocellular part of the pregeniculate, the ventromedial hypothalamic nucleus (VMH), the pretectum such as the anterior pretectal nucleus, the prosomere1 periaqueductal gray (p1PAG), the medial part of the retromammillary nucleus (RMM), the dorsal and ventral zona incerta (ZID/ZIV), the midbrain periaqueductal gray (PAG) including the lateral and ventrolateral parts, the reticular and other parts of the substantia nigra (SNR/SNC/SNL), the parvicellular and magnocellular parts of the red nucleus (RPC/RMC), the intermediate white layer of the superior colliculus (InWh), the external cortex of the inferior colliculus (ECIC), the mesencephalic reticular formation (mRt), the precuneiform nucleus (PrCnF), the medial raphe nucleus (MnR), the reticulotegmental nucleus of the pons (RtTg), the paralemniscal nucleus (PL), the oral pontine reticular nucleus (PnO), the ventral tegmental nucleus (VTg), the motor trigeminal nucleus (5 N), the abducens nucleus (6 N), the facial nucleus (7 N), the vagus nerve nucleus (10 N), the hypoglossal nucleus (12 N), the nucleus of roller (Ro), the beta part of the central gray (CGB), the locus coeruleus (LC), the principal sensory trigeminal nucleus (Pr5), the oral, intermediate, and caudal parts of the spinal trigeminal nuclei (Sp5O/Sp5I/Sp5C), the medial, superior, lateral, and spinal vestibular nuclei (MVe/SuVe/LVe/SpVe), the prepositus nucleus (Pr), the dorsal cochlear nucleus (DC), the external cuneate nucleus (ECu), the gigantocelluar reticular nuclei including the dorsal paragigantocellular reticular nucleus (DPGi), the gigantocellular nucleus (Gi), the alpha, ventral parts of the gigantocellular reticular nuclei (GiA/GiV), lateral paragigantocellular reticular nucleus (LPGi); the intermediate reticular nucleus (IRt), the linear nucleus of the hindbrain (Li), the lateral reticular nucleus (LRt), the pre-Botzinger complex/caudoventrolateral reticular nucleus (PrBo/CVL), the dorsal and ventral medullary reticular nuclei (MdD/MdV), the solitary nucleus (Sol). The *scale bar* is 800 μm in **a**, **b**, **j**, **k**, **m**; 900 μm in **c–e**, **g–i**; 1 mm in **f** and **l**; and 400 μm in **n–r**

nucleus had more positive cells in its middle portion, and the medial vestibular nucleus mainly had positive cells in its parvicellular portion (Fig. 2m–p). In the reticular formation, except for the alpha part of the gigantocellular reticular nucleus and the lateral paragigantocellular reticular nucleus, positive cells were mainly sporadically distributed (Fig. 3k–n).

In the spinal cord, not only motor neurons but also interneurons in laminae 7 and 8 in the ventral horn expressed SEIPIN. In the dorsal horn; the majority of SEIPIN-positive neurons were in laminae 3–6. The area surrounding the central canal (lamina 10) also had a small number of SEIPIN-positive neurons (Fig. 3o, p).

Double labeling with anti-NeuN and anti-SEIPIN showed that all SEIPIN-expressing cells in the red nucleus, substantia nigra, and paraventricular hypothalamic nucleus were neurons (Fig. 4). In other brain areas, close to all SEIPIN-positive cells were neurons.

In the retrograde study, areas for motor control including the motor and somatosensory cortices, the red nucleus, the hindbrain reticular formation, the vestibular complex, the subcoeruleus nucleus, the raphe nuclei, and the paralemniscal nucleus had SEIPIN-positive neurons which also projected to the spinal cord (Fig. 5).

Discussion

The present study mapped the expression pattern of SEIPIN in the mouse central nervous system using immunohistochemical staining. While the majority of SEIPIN-expressing regions that were observed were similar to those reported by the in situ hybridization study (Garfield et al. 2012), a number of areas have not been reported before. They include: the auditory and dorsal/intermediate endopiriform cortices which have low to moderate levels of SEIPIN; the ectorhinal and the perirhinal cortices, which have moderate to high levels of SEIPIN; the cortex-amygdala transition zone, the basomedial amygdaloid nucleus, anterior cortical amygdaloid nucleus, extension of the amygdala, and posterolateral/posteromedial cortical amygdaloid area, which have either low or low to moderate levels of SEIPIN; the accumbens nucleus, especially the shell region, which has low to moderate levels of SEIPIN; the interstitial nucleus of the posterior limb of the anterior commissure, which has low levels of SEIPIN; the dorsal tenia tecta, which has moderate to high levels of SEIPIN; the caudate putamen, which has a small number of SEIPIN-positive cells which are widely spread within this nucleus; the dorsal lateral geniculate nucleus, which has a number of positive cells, although they are lightly labeled; the retromammillary nucleus, especially its medial part, which has moderate levels of SEIPIN; the lithoid nucleus, which has low to moderate levels of SEIPIN; and lastly the oculomotor and trochlear nuclei, which have moderate numbers of SEIPIN-positive cells.

The in situ hybridization study thoroughly examined Bscl2 gene expression in the mouse brain, but the technique has its limitations. In particular, those weakly positive or a small number of positive cells might be missed in

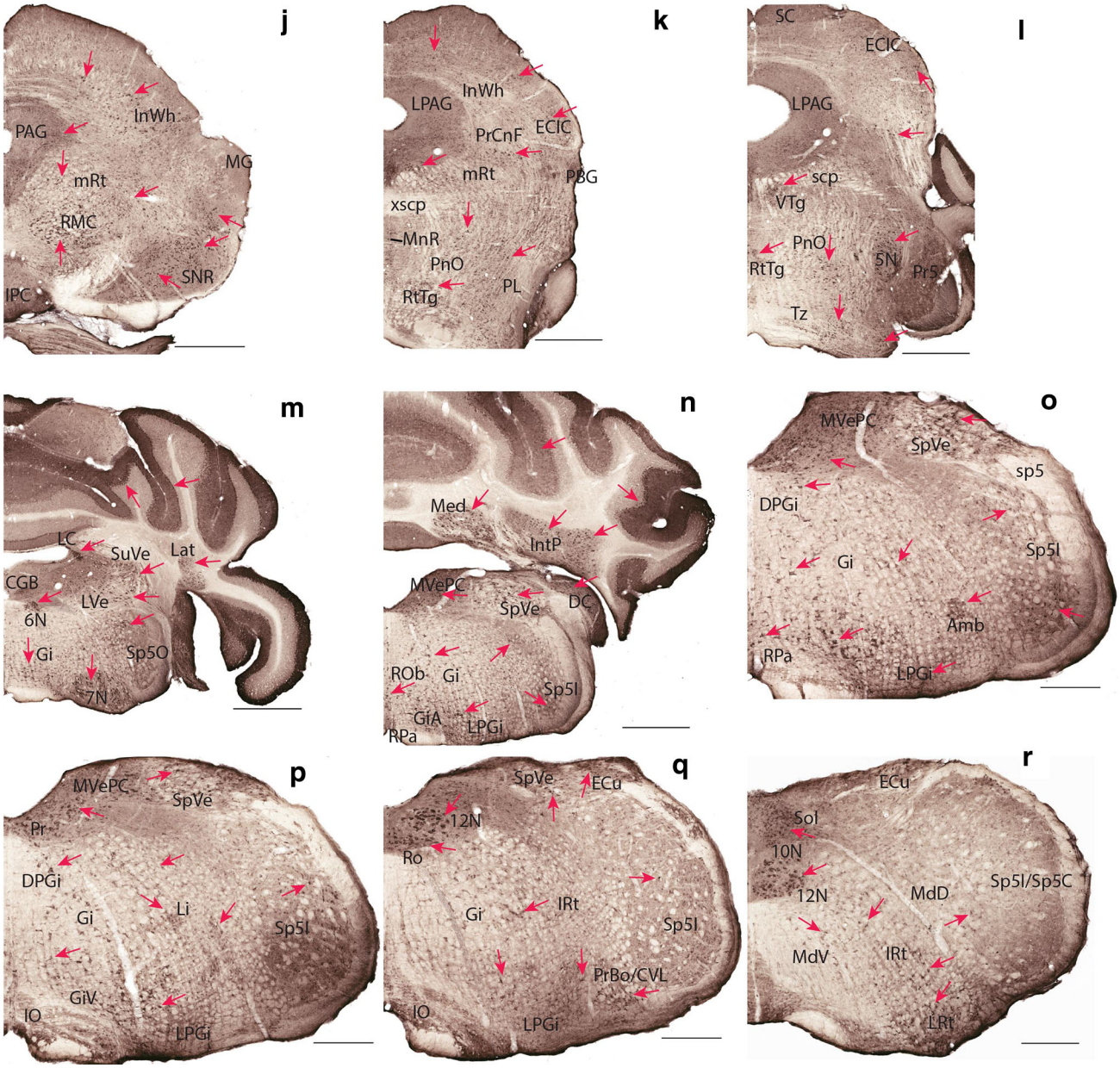

Fig. 2 continued

data analysis. For example, Northern blot has shown that there is expression of the Bscl2 gene in the caudate putamen (Windpassinger et al. 2004), but in situ hybridization did not show this (Garfield et al. 2012). The use of SEIPIN antibody has the advantage of detecting all SEIPIN-positive cells throughout the brain although they may be sparsely distributed.

Garfield and colleagues used in situ hybridization to map the location of Bscl2 mRNA-positive cells and described the intensity of the Bscl2 expression level. The present study focused on the location and the number of cells that were positive for anti-SEIPIN. This study demonstrated that there is an important difference between the results generated from these two techniques. However, it is possible that they are complementary. For example, the majority of the cortical areas were reported to have very low levels of Bscl2 mRNA in the in situ hybridization study, but the present study shows a large number of positive cells in these regions.

The motor cortex has been associated with motor deficits in Bscl2 mutant patients (Windpassinger et al. 2004; Ito and Suzuki 2009; Yagi et al. 2011; Guillén-Navarro et al. 2013), and SEIPIN expression in neurons of the motor cortex is consistent with this theory. However, a

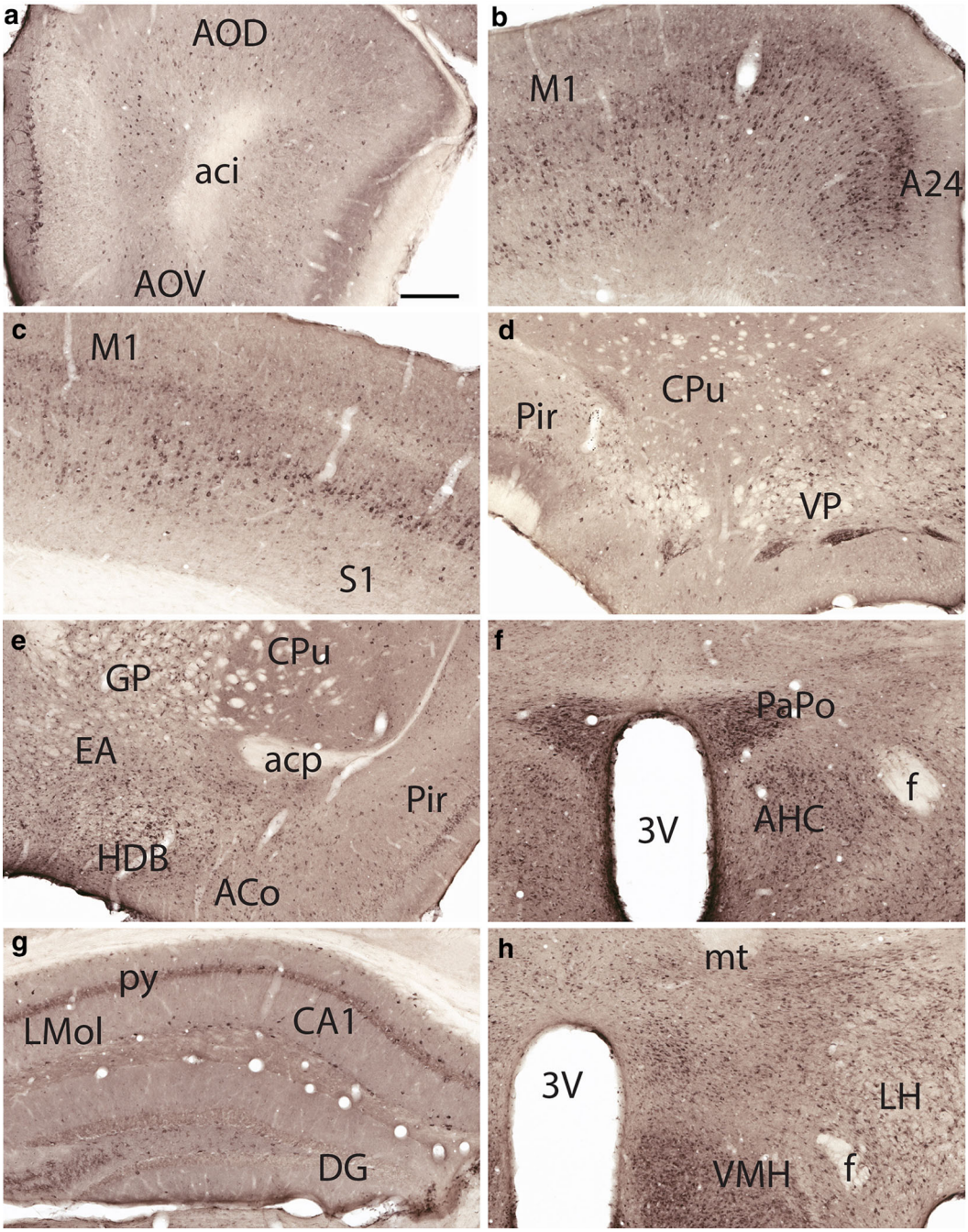

Fig. 3 Expression of SEIPIN in the mouse brain and spinal cord under 100× magnification. **a** SEIPIN-positive cells in the anterior olfactory nucleus. **b** SEIPIN-positive cells in the rostral motor cortex and A24. Note the gap between positive cells in layer 4 and 6 in M1. **c** SEIPIN-positive cells in M1 and S1. Note S1 has few cells in layer 6. **d** SEIPIN-positive cells in the ventral part of CPu and the ventral pallidum. **e** SEIPIN-positive cells in the caudate putamen (CPu), globus pallidus (GP), extension of amygdala (EA), nucleus of the horizontal limb of the diagonal band (HDB), the piriform cortex (Pir), and the anterior cortical amygdaloid nucleus (ACo). **f** SEIPIN-positive cells in the anterior hypothalamic nucleus (AHC), posterior paraventricular nucleus (PaPo), and the lateral hypothalamus (LH). **g** SEIPIN-positive cells in the hippocampus. Most cells are either on the surface or in the central part of each layer. **h** SEIPIN-positive cells in LH, VMH, and the dorsomedial hypothalamic nucleus (DM). **i** SEIPIN-positive cells in SNR and SNC. **j** SEIPIN-positive cells in RMC and 3 N. **k** SEIPIN-positive cells in 5 N and 5ADi, and to a lesser extent, in the caudal pontine reticular nucleus (PnC), and the subcoeruleus nucleus (SubC). **l** SEIPIN-positive cells in 7 N, and to a lesser extent, in Gi, GiA, and raphe magnus nucleus (RMg). **m** SEIPIN-positive cells in Amb, and the reticular formation including Gi, GiV, LPGi, IRt. **n** SEIPIN-positive cells in Li and the reticular formation including Gi, GiV, LPGi, IRt. **o** SEIPIN-positive cells in the dorsal horn of the spinal cord. **p** SEIPIN-positive cells in the ventral horn of the spinal cord. The *scale bar* is 200 μm

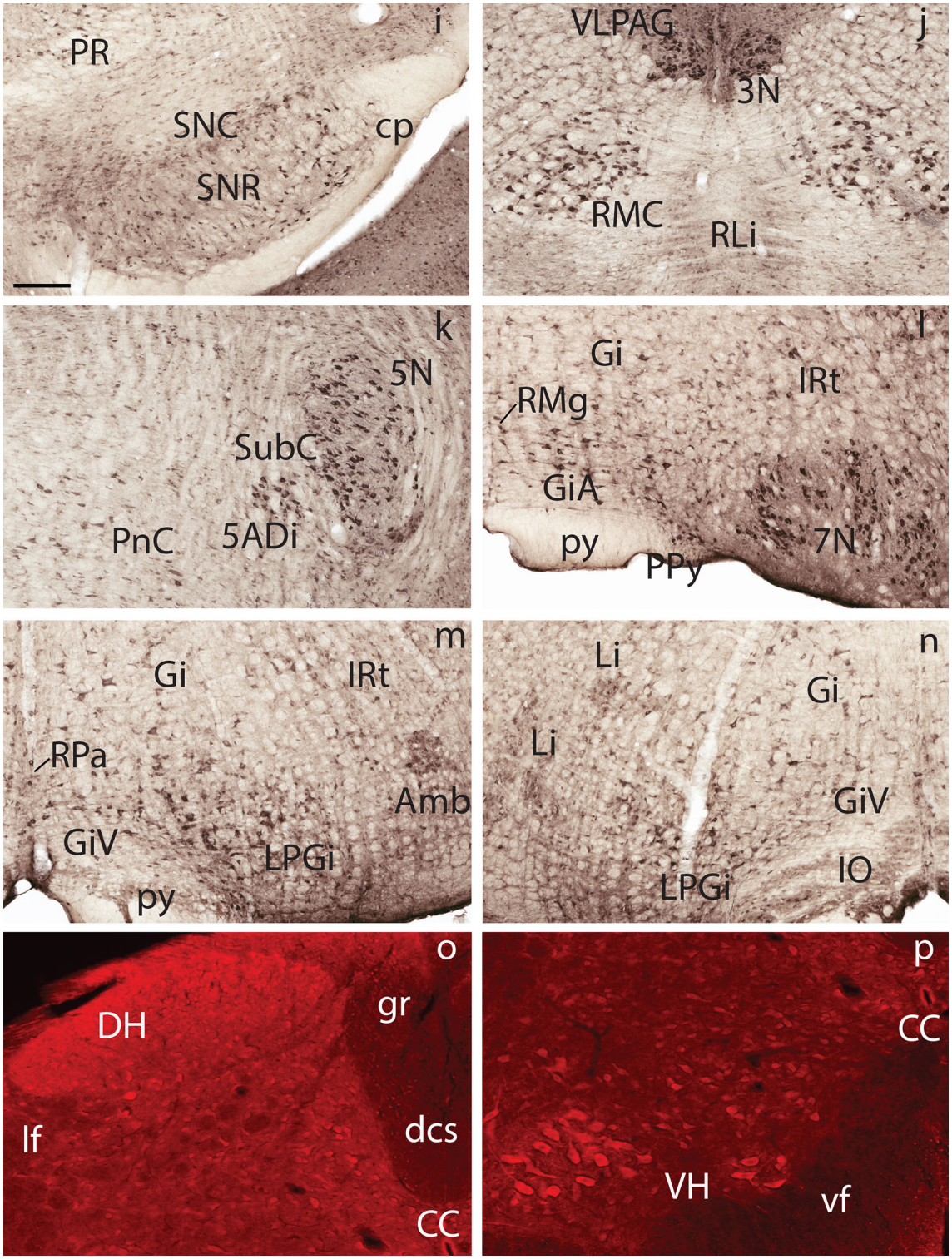

Fig. 3 continued

large number of SEIPIN-positive cells were also found in the somatosensory, visual, auditory, and cingulate cortices. It is possible that cells in the somatosensory cortex are involved in motor control, particularly as they were found to project to the spinal cord (Liang et al. 2011). Consistent with this concept is that, in the present study, some neurons in both the motor and somatosensory cortices that were SEIPIN positive, were retrogradely labeled by tracer

Table 2 Abbreviations of brain areas

3 V: 3rd ventricle
3 N: Oculomotor nu
4 N: Trochlear nu
5ADi: Motor trigeminal nu, anterior digastric part
5 N: Motor trigeminal nu
6 N: Abducens nu
7 N: Facial nu
10 N:Vagus nerve nu
12 N: Hypoglossal nu
A24: Cingulate cortex, area 24
A24b: Cingulate cortex, area 24b
A29: Cingulate cortex, area 29
A29c: Cingulate cortex, area 29c
A30: Cingulate cortex, area 30
A32: Cingulate cortex, area 32
AA: Anterior amygdaloid area
aca: Anterior commissure, anterior part
AcbC: Accumbens nu, core
AcbSh: Accumbens nu, shell
aci: Anterior commissure, intrabulbar part
ACo: Anterior cortical nu of amygdala
acp: Anterior commissure, posterior limb
AD: Anterodorsal nu
AHA: Anterior hypothalamic area, anterior part
AHC: Anterior hypothalamic area, central part
AHiPM: Amygdalohippocampal area, posteromedial part
AHP: Anterior hypothalamic area, posterior part
AID: Agranular insular cortex, dorsal part
AIV: Agranular insular cortex, ventral part
Amb: Ambiguus nu
AOD: Anterior olfactory area, dorsal part
AOL: Anterior olfactory nu, lateral part
AOM: Anterior olfactory nu, medial part
AOV: Anterior olfactory area, ventral part
AP: Area postrema
APT: Anterior pretectal nu
Arc: Arcuate hypothalamic nu
Au1: Primary auditory cortex
AuD: Secondary auditory cortex, dorsal part
AuV: Secondary auditory cortex, ventral part
AV: Anteroventral thalamic nu
Bar: Barrington's nu
BIC: Nu of the brachium of the inferior colliculus
BLA: Basolateral amygdaloid nu, anterior part
BMA: Basomedial amygdaloid nu, anterior part
CA1: Field CA1 of the hippocampus
CAT: Nu of the central acoustic tract
CeM: Central amygdaloid nu, medial part
CeL: Central amygdaloid nu, lateral part
CGB: Central gray, beta part

Table 2 continued

Cl: Claustrum
CL: Centrolateral thalamic nu
CLi: Caudal linear nu of the raphe
cp: Cerebral peduncle
CPu: Caudate putamen
CVL: Caudoventrolateral reticular nu
CxA: Cortex-amygdala transition zone
DA: Dorsal hypothalamic area
DC: Dorsal cochlear nu
DEn: Dorsal endopiriform nu
DG: Dentate gyrus
DH: Dorsal horn
DI: Dysgranular insular cortex
Dk: Nu of Darkschewitsch
DLEnt: Dorsolateral entorhinal cortex
DLG: Dorsal lateral geniculate nu
DLO: Dorsolateral orbital cortex
DM: Dorsomedial hypothalamic nu
DpG: Deep gray layer of the superior colliculus
DPGi: Dorsal paragigantocellular nu
DR: Dorsal raphe nu
DTT: Dorsal tenia tecta
EA: Extension of the amygdala
ECIC: External cortex of the inferior colliculus
ECu: External cuneate nu
Ect: Ectorhinal cortex
EP: Entopeduncular nu
ER: Endoplasmic reticulum
EW: Edinger–Westphal nu
f: Fornix
F: Nu of the fields of Forel
FG: Fluoro-gold
fi: Fimbria
fr: Fasciculus retroflexus
Fr3: Frontal cortex, area 3
FrA: Frontal association cortex
Gi: Gigantocellular reticular nu
GI: Granular insular cortex
GiA: Gigantocellular reticular nu, alpha part
GiV: Gigantocellular reticular nu, ventral part
GP: Globus pallidus
HDB: Nu of the horizontal limb of the diagonal band
Hip: Hippocampus
ic: Internal capsule
IEn: Intermediate endopiriform nu
IntA: Interposed cerebellar nu, anterior part
IntP: Interposed cerebellar nu, posterior part
InWh: Intermediate white layer of the superior colliculus
IO: Inferior olivary nu
IP: Interpeduncular nu

Table 2 continued

IPACL: Interstitial nu of the posterior limb of the anterior commissure, lateral part
IPACM: Interstitial nu of the posterior limb of the anterior commissure, medial part
IPC: Interpeduncular nu, caudal subnucleus
IRt: Intermediate reticular nu
LA: Lateral amygdaloid nu
Lat: Lateral cerebellar nu
LC: Locus coeruleus
LDB: Lateral nu of the diagonal band
LDDM: Laterodorsal thalamic nu, dorsomedial part
LDVL: Laterodorsal thalamic nu, ventrolateral part
LDTg: Laterodorsal tegmental nu
LH: Lateral hypothalamic area
Li: Linear nu of the hindbrain
LMol: Lacunosum molecular layer of the hippocampus
LO: Lateral orbital cortex
LOT: Nu of the lateral olfactory tract
LPAG: Lateral periaqueductal gray
LPB: Lateral parabrachial nu
LPGi: Lateral paragigantocellular nu
LPO: Lateral preoptic area
LRt: Lateral reticular nu
LSD: Lateral septal nu, dorsal part
LSI: Lateral septal nu, intermediate part
LSV: Lateral septal nu, ventral part
Lth: Lithoid nu
LVe: Lateral vestibular nu
M1: Primary motor cortex
M2: Secondary motor cortex
MA3: Medial accessory oculomotor nu
MCPC: Magnocellular nu of the posterior commissure
MD: Mediodorsal thalamic nu
MdD: Medullary reticular nu, dorsal part
MdV: Medullary reticular nu, ventral part
MeAD: Medial amygdaloid nu, anterodorsal part
MeAV: Medial amygdaloid nu, anteroventral part
Med: Medial cerebellar nucleus
MePD: Medial amygdaloid nu, posterodorsal part
MePV: Medial amygdaloid nu, posteroventral part
MG: Medial geniculate nu
MGV: Medial geniculate nu, ventral part
MiTg: Microcellular tegmental nu
MnR: Median raphe nu
MO: Medial orbital cortex
MPA: Medial preoptic area
MPB: Medial parabrachial nu
MPO: Medial preoptic nu
mRt: Mesencephalic reticular formation
MS: Medial septal nu

Table 2 continued

mt: Mammillothalamic tract
MVe: Medial vestibular nu
MVePC: Medial vestibular nu, parvicellular part
OPC: Oval paracentral thalamic nu
p1PAG: Prosomere 1 periaqueductal gray
p1Rt: Prosomere 1 reticular formation
Pa4: Paratrochlear nu
PaAP: Paraventricular hypothalamic nu, anterior parvicellular part
PAG: Periaqueductal gray
PaDC: Paraventricular hypothalamic nu, dorsal cap
PaF: Parafascicular thalamic nu
PaLM: Paraventricular hypothalamic nu, lateral magnocellular part
PaMP: Paraventricular hypothalamic nu, medial parvicellular part
PaPo: Paraventricular hypothalamic nu, posterior part
PBG: Parabigeminal nu
PC: Paracentral thalamic nu
PCRt: Parvicellular reticular nu
PDTg: Posterodorsal tegmental nu
Pe: Periventricular hypothalamic nu
PH: Posterior hypothalamic nu
PIF: Parainterfascicular nu of the ventral tegmental area
Pir: Piriform cortex
PL: Paralemniscal nu
PLCo: Posterolateral cortical amygdaloid area
PMCo: Posteromedial cortical amygdaloid area
PMD: Premammillary nu, dorsal part
PMnR: Paramedian raphe nu
PMV: Premammillary nu, ventral part
Pn: Pontine nu
PnO: Pontine reticular nu, oral part
PnC: Pontine reticular nu, caudal part
Po: Posterior thalamic nu
PPy: Parapyramidal nu
Pr: Prepositus nu
PR: Prerubral field
Pr5: Principal trigeminal nu
PrBo: Pre-Botzinger complex
PrC: Precommissural nu
PrCnF: Precuneiform nu
PrGMC: Pregeniculate nu of the prethalamus, magnocellular part
PRh: Perirhinal cortex
PVA: Paraventricular thalamic nu, anterior part
PVP: Paraventricular thalamic nu, posterior part
py: Pyramidal tract
Py: Pyramidal cell layer of the hippocampus
RChL: Retrochiasmatic area, lateral part
Re: Reuniens nu
RLi: Rostral linear nu of the raphe
RMC: Red nu, magnocellular part

Table 2 continued

RMg: Raphe magnus nu
RMM: Retromammillary nu, medial part
RML: Retromammillary nu, lateral part
Ro: Nu of roller
ROb: Raphe obscurus nu
RPa: Raphe pallidus nu
RPC: Red nu, parvicellular part
RPF: Retroparafascicular nu
Rt: Reticular nu of the thalamus
RtTg: Reticulotegmental nu of pons
S1: Primary somatosensory cortex
S1DZ: Primary somatosensory cortex, dysgranular zone
S1FL: Primary somatosensory cortex, forelimb region
S1J: Primary somatosensory cortex, jaw region
S1ULp: Primary somatosensory cortex, upper lip region
SC: Superior colliculus
SChDL: Suprachiasmatic nu, dorsolateral part
scp: Superior cerebellar peduncle
SGe: Supragenual nu
SHy: Septohypothalamic nu
SIB: Substantia innominate, basal part
sm: Stria medullaris
SN: Substantia nigra
SNC: Substantia nigra, compact part
SNL: Substantia nigra, lateral part
SNR: Substantia nigra, reticular part
Sol: Solitary nu
sp5: Spinal trigeminal tract
Sp5C: Spinal trigeminal nu, caudal part
SPF: Subparafascicular thalamic nu
Sp5O: Spinal trigeminal nu, oral part
Sp5I: Spinal trigeminal nu, interpolar part
SpVe: Spinal vestibular nu
STh: Subthalamic nu
STLD: Bed nu of the stria terminalis, lateral division
STLJ: Bed nu of the stria terminalis, lateral division, juxtacapsular part
STLP: Bed nu of the stria terminalis, lateral division, posterior part
STMA: Bed nu of the stria terminalis, medial division, anterior part
Sub: Submedius thalamic nu
SubB: Subbrachial nu
SubC: Subcoeruleus nu
SubG: Subgeniculate nu of prethalamus
SuVe: Superior vestibular nu
TeA: Temporal association cortex
Tz: Nu of the trapezoid body
V1: Primary visual cortex
V2L: Secondary visual cortex, lateral area
V2ML: Secondary visual cortex, mediolateral area

Table 2 continued

V2MM: Secondary visual cortex, mediomedial area
VDB: Nu of the vertical limb of the diagonal band
VeCb: Vestibulocerebellar nu
VL: Ventrolateral thalamic nu
VLPAG: Ventrolateral periaqueductal gray
VM: Ventromedial thalamic nu
VMH: Ventromedial hypothalamic nu
VMHC: Ventromedial hypothalamic nu, central part
VMHDM: Ventromedial hypothalamic nu, dorsomedial part
VMHVL: Ventromedial hypothalamic nu, ventrolateral part
VO: Ventral orbital cortex
VP: Ventral pallidum
VPL: Ventral posterolateral thalamic nu
VPM: Ventral posteromedial thalamic nu
VTg: Ventral tegmental nu
VTT: Ventral tenia tecta
Xi: Xiphoid thalamic nu
xscp: Decussation of the superior cerebellar peduncle
ZI: Zona incerta
ZID: Zona incerta, dorsal part

injection into the spinal cord. This indicates that SEIPIN-positive neurons in the cortex are likely to be involved in motor control, and could explain the pyramidal signs experienced by patients with a Bscl2 mutation. SEIPIN-positive cells were found in other motor related nuclei including the caudate putamen, globus pallidus, substantia nigra, subthalamic nucleus, hypothalamic nuclei (such as ventromedial and dorsomedial hypothalamic nuclei), reticular formation in the brainstem, and the red nucleus. Some of these nuclei project to the spinal cord, in particular the red nucleus, and the hindbrain reticular formation, with their fiber terminals being shown to terminate on motor neurons in the mouse spinal cord (Liang et al. 2012, 2015). However, these cells have not been tested for their involvement in motor control in previous studies. In terms of SEIPIN expression in motor neurons of the spinal cord, it is plausible to assume that these neurons are responsible for the atrophy of the limb muscles as described by Silver (1966).

Some patients with motor neuropathy also showed eye movement deficits. Garfield et al. (2012) tried to explain this by the presence of Bscl2 in the optic, oculomotor, and the trochlear nuclei but failed to reveal the expression of this gene in these nuclei. However, the present study found a cluster of strongly positive cells in both the oculomotor and the trochlear nuclei. Whether this difference is due to the method or truly due to the presence of SEIPIN in these nuclei is still unclear. It has been noted in patients a high prevalence of mild mental retardation (Agarwal et al. 2003)

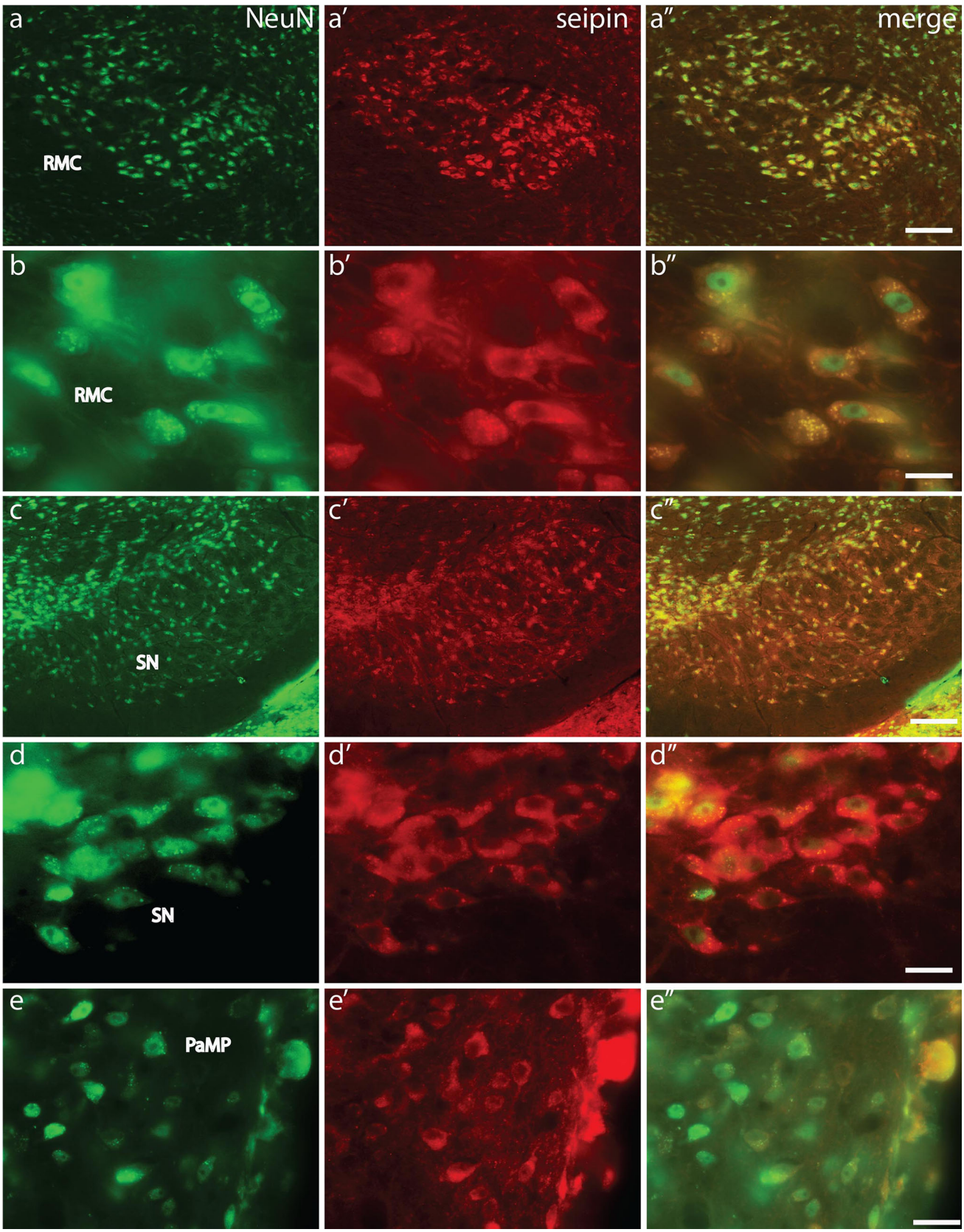
a
NeuN
a′
seipin
a″
merge
RMC
b
b′
b″
RMC
c
c′
c″
SN
d
d′
d″
SN
e
e′
e″
PaMP

◀**Fig. 4** Double labeling with NeuN and SEIPIN antibodies in the magnocellular part of the red nucleus (RMC, **a**–**b**″), the substantia nigra (SN, **c**–**d**″), and the medial parvicellular part of the paraventricular nucleus (PaMP, **e**–**e**″). The *scale bar* is 100 μm in **a**–**a**″ and **c**–**c**″ and 50 μm in **b**–**b**″, **d**–**d**″, and **e**–**e**″

and in male knockout mice depression/anxiety-like behaviors (Zhou et al. 2014), these symptoms might be explained by the expression of SEIPIN in cortical areas, the ventral forebrain, and the amygdala. Strong SEIPIN expression in the paraventricular hypothalamic nucleus, the arcuate and solitary nuclei may indicate the possible involvement of SEIPIN in eating behaviors and the central control of lipid metabolism.

In the in situ hybridization study, the medial vestibular nucleus was shown to express Bscl2 mRNA. Lateral to this nucleus, the spinal vestibular nucleus also had a strong

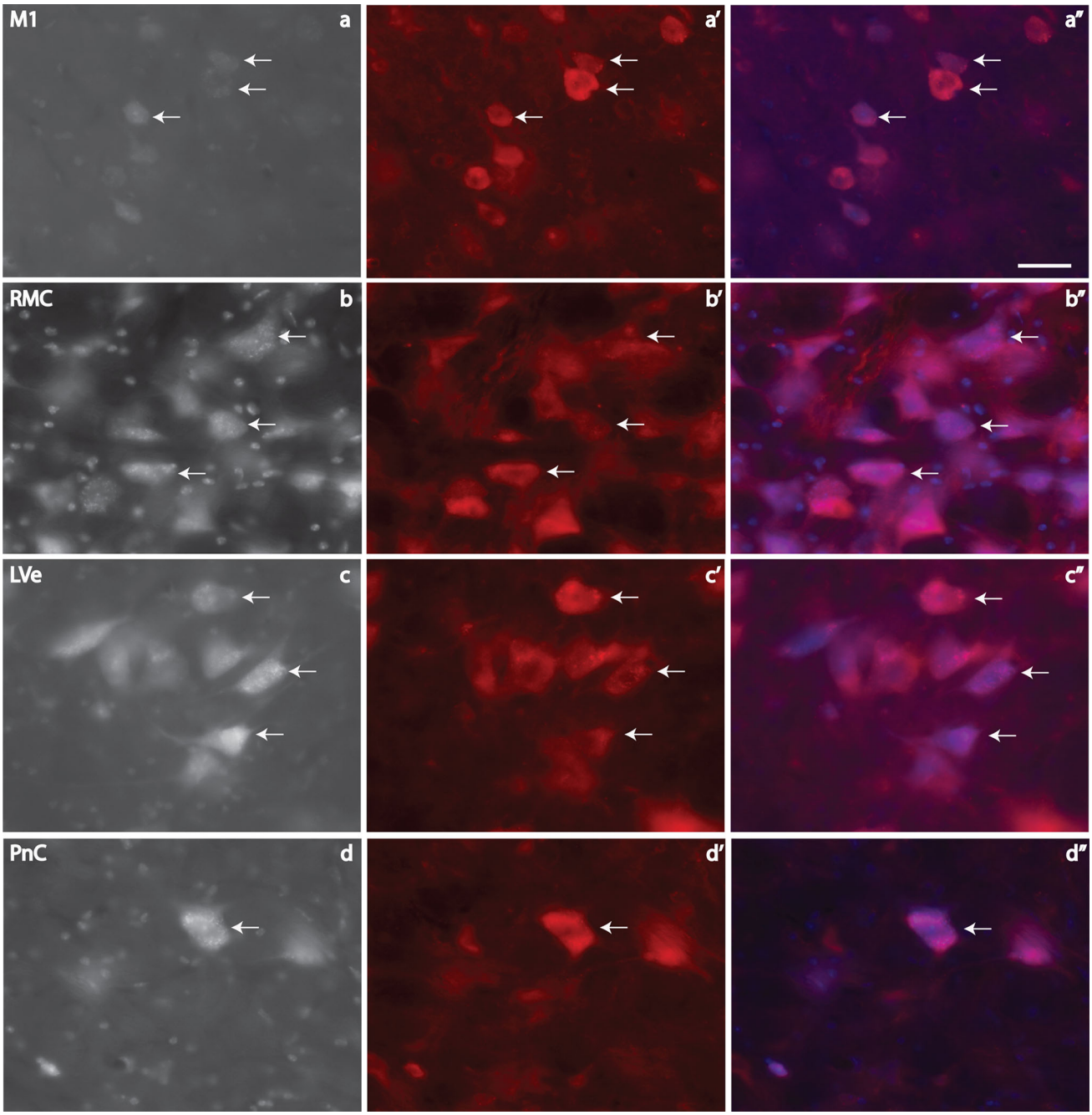

Fig. 5 Immunofluorescent staining for SEIPIN on fluoro-gold labeled neurons. **a**–**d** Double labeling on neurons in the M1, RMC, LVe, and PnC. The *left column* shows FG labeled neurons, the *middle column* shows SEIPIN-positive cells, and the *right column* shows the merged images. The *arrows* point to the double labeled neurons. The *scale bar* is 50 μm

signal, indicating the presence of Bscl2 mRNA in this nucleus (Garfield et al. 2012). Rostral to these two nuclei, the other divisions of the vestibular complex also contained SEIPIN-positive cells although there were only a small number. Some of these neurons also projected to the spinal cord, especially those in the lateral vestibular nucleus. The significance of SEIPIN expression in the vestibular complex is unclear because patients with Bscl2 mutations do not show balance problems.

Although motor neurons in both the cortex and the spinal cord express SEIPIN, they are not necessarily involved in the pathogenesis of motor neuropathy. For example, Irobi et al. (2004) reported that some patients have spasticity and distal amyotrophy in the lower limbs and pyramidal signs, whereas other patients do not have pyramidal signs. This suggests that motor neurons in the spinal cord are comparatively more vulnerable than those in the cortex. In a report by Cafforio et al. (2008), it was shown using MRI that a patient with a Bscl2 gene mutation had pyramidal tract alteration. Another interesting observation was that in one affected family the upper limbs were involved first, but that this was not the case in other families, indicating that the natural history of the disorder does not have a fixed pattern.

Limitations of the present study

The present study found more nuclei positive for SEIPIN than the previous in situ hybridization study. However, there are also some nuclei which we have not reported to be positive for SEIPIN but were reported to be positive in the in situ hybridization study (Garfield et al. 2012). These include the olfactory tubercle, the subfornical organ, the medial mammillary nucleus. They are all close to the brain surface or the ventricle; it is likely that there is an edge effect for the immunohistochemical staining. Though we have seen the dark signal, we did not report these nuclei because we could not differentiate them from the background staining. The other limitation is that positive neurons are present in many nuclei of the brain. It is not certain which nuclei are more important for motor deficit in the mouse model or patient with gene mutations. This will require further investigations to confirm the role of each nucleus in the manifestations of patients with Bscl2 gene mutations or deletions.

Conclusion

In this study, SEIPIN was found to be widely expressed in the central nervous system of the mouse with SEIPIN-positive neurons found in the motor and somatosensory cortex, red nucleus, and hindbrain reticular formation. All these regions project to the cervical cord in the mouse. This might help to explain the clinical manifestations of a dysfunctional SEIPIN protein.

Acknowledgments This work was supported by the Australian Research Council Centre of Excellence for Integrative Brain Function (ARC Centre Grant CE140100007) and a project grant (1027387) from the National Health and Medical Research Council of Australia. H. Yang is a Senior Research Fellow of the NHMRC. We appreciate Dr Emma Schofield's help in proof reading this manuscript.

Compliance with ethical standards

Conflict of interest The authors declare that there is no conflict of interests.

Ethical approval All procedures were in compliance with the ethical standards of the Animal Care and Ethics Committee of The University of New South Wales.

References

Agarwal AK, Simha V, Oral EA, Moran SA, Gorden P et al (2003) Phenotypic and genetic heterogeneity in congenital generalized lipodystrophy. J Clin Endocrinol Metab 88:4840–4847

Cafforio G, Calabrese R, Morelli N, Mancuso M, Piazza S, Martinuzzi A, Bassi MT, Crippa F, Siciliano G (2008) The first Italian family with evidence of pyramidal impairment as phenotypic manifestation of Silver syndrome BSCL2 gene mutation. Neurol Sci 29(3):189–191

Cui X, Wang Y, Tang Y, Liu Y, Zhao L, Deng J, Xu G, Peng X, Ju S, Liu G, Yang H (2011) Seipin ablation in mice results in severe generalized lipodystrophy. Hum Mol Genet 20(15): 3022–3030

Ebihara K, Kusakabe T, Masuzaki H, Kobayashi N, Tanaka T, Chusho H, Miyanaga F, Miyazawa T, Hayashi T, Hosoda K, Ogawa Y, Nakao K (2004) Gene and phenotype analysis of congenital generalized lipodystrophy in Japanese: a novel homozygous nonsense mutation in SEIPIN gene. J Clin Endocrinol Metab 89(5):2360–2364

Fei W, Du X, Yang H (2011) Seipin, adipogenesis and lipid droplets. Trends Endocrinol Metab 22(6):204–210

Garfield AS, Chan WS, Dennis RJ, Ito D, Heisler LK, Rochford JJ (2012) Neuroanatomical characterisation of the expression of the lipodystrophy and motor-neuropathy gene Bscl2 in adult mouse brain. PLoS ONE 7(9):e45790

Guillén-Navarro E, Sánchez-Iglesias S, Domingo-Jiménez R, Victoria B, Ruiz-Riquelme A, Rábano A, Loidi L, Beiras A, González-Méndez B, Ramos A, López-González V, Ballesta-Martínez MJ, Garrido-Pumar M, Aguiar P, Ruibal A, Requena JR, Araújo-Vilar D (2013) A new SEIPIN-associated neurodegenerative syndrome. J Med Genet 50(6):401–409

Guo J, Qiu W, Soh SL, Wei S, Radda GK, Ong WY, Pang ZP, Han W (2013) Motor neuron degeneration in a mouse model of SEIPINopathy. Cell Death Dis 4:e535

Irobi J, Van den Bergh P, Merlini L et al (2004) The phenotype of motor neuropathies associated with BSCL2 mutations is broader than Silver syndrome and distal HMN type V. Brain 127:2124–2130

Ito D, Suzuki N (2007) Molecular pathogenesis of SEIPIN/BSCL2-related motor neuron diseases. Ann Neurol 61:237–250

Ito D, Suzuki N (2009) SEIPINopathy: a novel endoplasmic reticulum stress associated disease. Brain 132:8–15

Ito D, Fujisawa T, Iida H, Suzuki N (2008a) Characterization of SEIPIN/BSCL2, a protein associated with spastic paraplegia 17. Neurobiol Dis 31:266–277

Ito D, Fujisawa T, Iida H, Suzuki N (2008b) Characterization of SEIPIN/BSCL2, a protein associated with spastic paraplegia 17. Neurobiol Dis 31(2):266–277

Jiang M, Gao M, Wu C, He H, Guo X, Zhou Z, Yang H, Xiao X, Liu G, Sha J (2014) Lack of testicular seipin causes teratozoospermia syndrome in men. Proc Natl Acad Sci USA 111(19):7054–7059

Liang H, Paxinos G, Watson C (2011) Projections from the brain to the spinal cord in the mouse. Brain Struct Funct 215(3–4): 159–186

Liang H, Paxinos G, Watson C (2012) The red nucleus and the rubrospinal projection in the mouse. Brain Struct Funct 217(2): 221–232

Liang H, Watson C, Paxinos G (2015) Terminations of reticulospinal fibers originating from the gigantocellular reticular formation in the mouse spinal cord. Brain Struct Funct. doi:10.1007/s00429-015-0993-z

Lundin C, Nordström R, Wagner K, Windpassinger C, Andersson H, von Heijne G, Nilsson I (2006) Membrane topology of the human SEIPIN protein. FEBS Lett 580(9):2281–2284

Magre J, Delepine M, Khallouf E et al (2001) Identification of the gene altered in Berardinelli-Seip congenital lipodystrophy on chromosome 11q13. Nat Genet 28:365–370

Paxinos G, Franklin KBJ (2013) The mouse brain in stereotaxic coordinates, 4th edn. Elsevier, San Diego

Sengul G, Watson C, Tanaka I, Paxinos G (2012) Atlas of the spinal cord of the rat, mouse, marmoset, rhesus, and human. Elsevier, San Diego

Silver JR (1966) Familial spastic paraplegia with amyotrophy of the hands. Ann Hum Genet 30:69–75

Wei S, Soh SL, Qiu W, Yang W, Seah CJ, Guo J, Ong WY, Pang ZP, Han W (2013) SEIPIN regulates excitatory synaptic transmission in cortical neurons. J Neurochem 124:478–489

Wei S, Soh SL, Xia J, Ong WY, Pang ZP, Han W (2014) Motor neuropathy-associated mutation impairs SEIPIN functions in neurotransmission. J Neurochem 129(2):328–338

Windpassinger C, Wagner K, Petek E, Fischer R, Auer-Grumbach M (2003) Refinement of the Silver syndrome locus on chromosome 11q12-q14 in four families and exclusion of eight candidate genes. Hum Genet 114(1):99–109

Windpassinger C, Auer-Grumbach M, Irobi J et al (2004) Heterozygous missense mutations in BSCL2 are associated with distal hereditary motor neuropathy and Silver syndrome. Nat Genet 36:271–276

Yagi T, Ito D, Nihei Y, Ishihara T, Suzuki N (2011) N88S SEIPIN mutant transgenic mice develop features of SEIPINopathy/BSCL2-related motor neuron disease via endoplasmic reticulum stress. Hum Mol Genet 20:3831–3840

Zhou L, Yin J, Wang C, Liao J, Liu G, Chen L (2014) Lack of SEIPIN in neurons results in anxiety- and depression-like behaviors via down regulation of PPARγ. Hum Mol Genet 23(15):4094–4102